

# Towards an Improved Uniform Color Space

Rolf G. Kuehni

DyStar L. P., 9844A Southern Pine Blvd., Charlotte, NC 28226

Received 24 October 1998; accepted 4 January 1999

*Abstract: Analysis of the Munsell, the OSA-UCS, and the NCS systems shows that the idea, originally introduced with the Adams–Nickerson color space and difference formula, that the Munsell value function not only applies to the tristimulus value Y but also to X and Z, is inaccurate. For all three systems, different power functions are required for X and Z. In the case of Z, different powers are needed for the yellow and blue halves. An additional correction is required for the curvature of the constant hue lines of blue colors. New a and b formulas are introduced that correct these shortcomings of CIELAB. In a hue scaling experiment with Munsell chips, the Munsell hue scale was found inaccurate, and a different number of equal-sized hue steps was found in some of the four quadrants. The implications for color difference calculation are discussed. © 1999 John Wiley & Sons, Inc. Col Res Appl, 24, 253–265, 1999*

*Key words: uniform color space; Munsell system; hue scaling; color difference calculation*

## INTRODUCTION

Of the two paradigms historically used for explaining the structure of global color space, accumulation of threshold color differences and construction from opponent-color dimensionalities, the latter has been historically more successful as a model for color difference and color-appearance calculation, despite its conceptual problems. In the former case, the global space is an accumulation of threshold differences (accumulation model).<sup>1</sup> In the latter case, the global space can be divided into smaller and smaller units until threshold is reached (division model).

Physical examples of the division model are the Munsell system, the OSA Uniform Color Space, and the NCS system. They all have been built according to different meth-

odologies. These systems (and possible others) contain structures that are common to them. The structures derive from the operation of an opponent-color system that is implicit in the CIE colorimetric system. A result of the functioning of this opponent-color system is the fact that changes in redness-greenness of object colors at a given lightness level change only the activity level of the  $\bar{x}$  color-matching function and changes in yellowness-blueness only that of the  $\bar{z}$  function, while lightness changes, by definition, change the activity of the  $\bar{y}$  function.

In 1976, the CIE recommended the CIELAB formulas as color space and color difference formulas “in the interest of promoting uniformity of usage.” These formulas are a minor modification of the Adams–Nickerson space and difference formulas, based in part on the Munsell system. When testing the CIELAB formula against the Munsell Renotation data, significant differences are found. Hue differences between Munsell samples at equal value and chroma differ up to a factor 3 when calculated with CIELAB, and there is a ratio of nearly 2:1 in chromas calculated for Munsell colors along the yellow–blue axis. In addition, CIELAB calculations are erroneous in their calculation of hue differences depending on the chroma of the colors.<sup>2</sup>

Relatively poor correlation between visual supra-threshold color difference judgments and calculated values have resulted in the development of the CMC and other similar color-difference formulas.<sup>3</sup> These are simple modifications of CIELAB that adjust CIELAB differences for adaptation effects due to the lightness and chroma of the surround (for gray surrounds), as well as correct hue differences in two ways: (a) presumed adjustment of the residual error of the CIELAB hue scale; (b) adjustment for the incorrect calculation by CIELAB of hue differences as a function of chroma. Except for the last item, fundamental flaws in CIELAB are not adjusted for by the CMC weights.

© 1999 John Wiley & Sons, Inc.

## WHAT CAUSES CHANGES IN HUE?

Zone theories describe changes in hue as a function of changes in opponent-color system activations. The CIELAB formula describes hue changes as changes in the ratios of the cube roots of the activations of the two opponent-color processes responsible for the creation of the hues in question. Thus, hue1 is determined by the ratio  $M1/M2$ , where  $M1, 2$  are values of opponent-color functions, and similarly for other hues. The ratio, and with it the hue, is independent of the magnitude of the function values and, therefore, of chroma. Visually, a hue can be described as an additive mixture of the two adjacent opponent-color processes. These processes have self-hues, described as the unique hues. They are visible in diluted form where the second system is not activated (or in balance); thus, the blue and yellow unique hues are visible where the redness-greenness system is in balance. They can be experimentally determined for object colors by picking them out of an array of color samples changing in hue only. Unique red, for example, is represented by the chip that is perceived as having neither a yellowish nor a bluish component. In such an experiment, color-normal observers pick unique hues with a narrow standard deviation. For example, from a series of Munsell chips at value 6 and chroma 8, fifteen observers picked on average 1.6R as the unique red with a standard deviation of 1.2 Munsell 100 Hue steps (see Table I).

Physical examples of unique hues, or innate knowledge

TABLE I. Experimentally determined uniform hue steps around the Munsell Hue circle at value 6 and chroma 8, based on the step 5PB to 10B as standard, expressed in Munsell 100 Hue steps.

Unique hue	Mean	Standard deviation	Distance <sup>a</sup>
B	5PB	0	5
	10B	0	5.4
	4.6B	1.25	4.5
	9.1BG	0.68	4.3
G	3.4BG	1.44	3.5
	6.9G	0.92	4.4
	1.3G	0.85	3.0
	7.5GY	1.02	3.7
	3.8GY	1.07	4.2
	9.6Y	0.83	4.6
Y	5Y	0.70	3.6
	1.4Y	1.08	5.8
	7.2YR	1.04	5.2
	2.4YR	0.98	5.3
R	7.7R	0.78	3.9
	1.6R	1.16	4.5
	6.1RP	0.76	3.1
	3.0RP	0.63	3.2
	9.8P	0.54	4.1
	5.7P	0.65	3.8
	1.9P	0.78	4.0
	7.9PB	0.63	4.6

<sup>a</sup> Distance to the following hue step.

of the unique hues can be used to estimate the content of two unique hues (the hue coefficients) in mixed hue samples. Such data have been reported by Indow,<sup>4</sup> by the

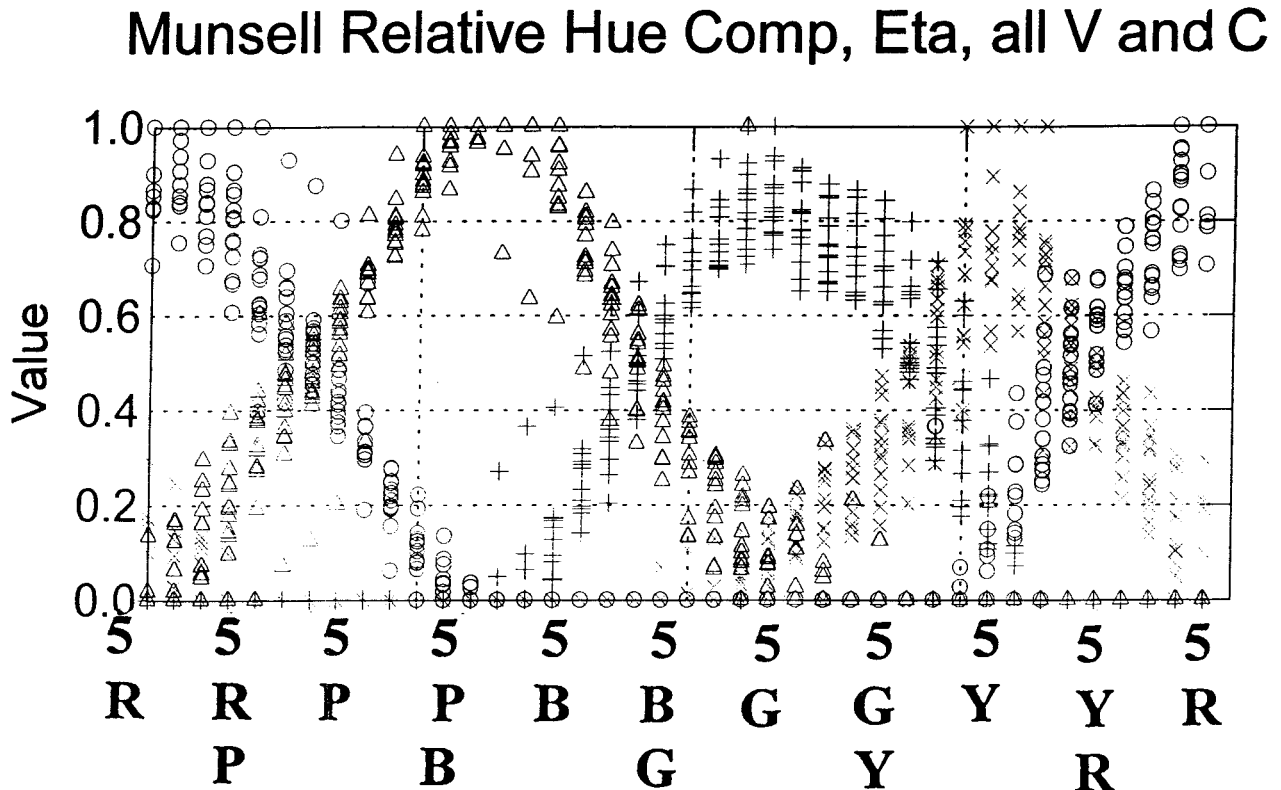


FIG. 1. Hue coefficient diagram as a function of Munsell hue. Each point represents average judgements of unique hue components of Munsell chips at all hues, values, and chromas. (See Ref. 4.)

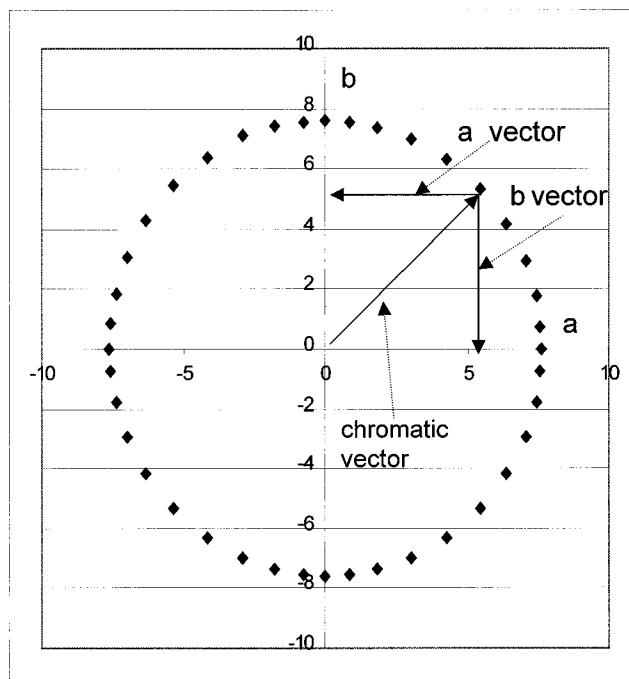


FIG. 2. Hypothetical hue circle showing the redness vector *a* and the yellowness vector *b* that together form the hue vector of the indicated color. The colors are equally spaced, based on equal changes in *a* and *b*.

creators of the NCS system,<sup>5</sup> and Kuehni.<sup>6</sup> Figure 1 shows the experimentally determined hue coefficients for Munsell colors at all values and chromas, reported by Indow. While showing scatter, there is also the indication of an orderly progression in the perceived content of the unique hues in mixed hues.

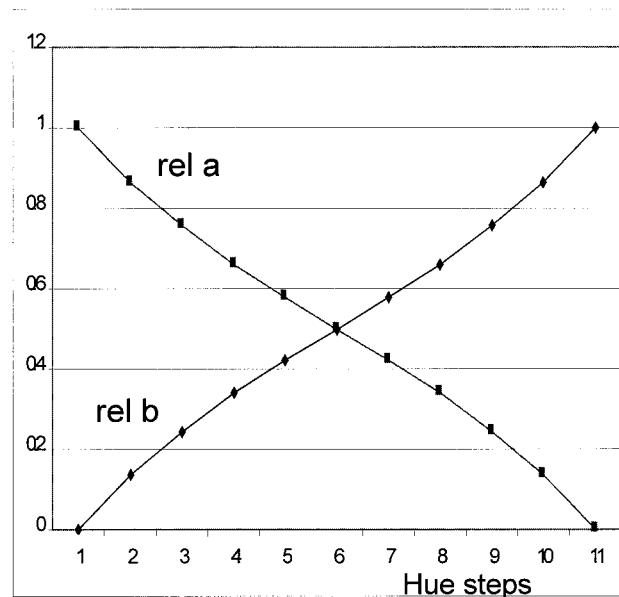


FIG. 3. Changes in hue coefficients *rel a* and *rel b* that result in ten equal hue increments in a quadrant, based on the hue changes resulting from equal changes in hue angle.

#### EQUAL HUE CHANGES: BASED ON A POLAR COORDINATE OR A CARTESIAN COORDINATE SYSTEM?

The question remains as to how equal-sized hue steps are caused. CIELAB and similar formulas imply a polar coordinate system, where equal calculated hue differences are not related to equal changes in the *a* and *b* axes, as they are in the Cartesian system. In the former, the increments change according to the sine function. In the latter, the following relationship applies:

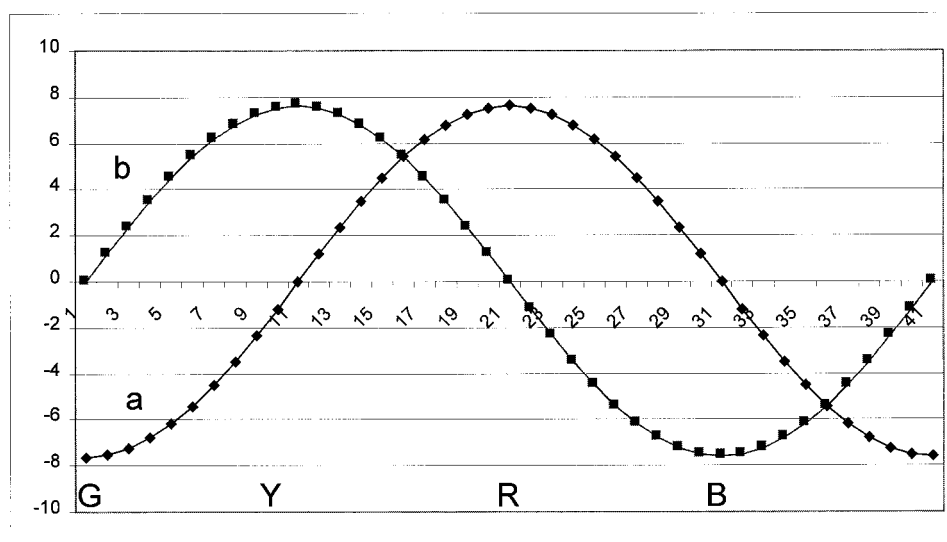


FIG. 4. Absolute chromatic vectors *a* and *b* required to obtain 40 equally spaced hues around the hue circle at a given level of chroma, based on the same model as Fig. 3. The capital letters indicate the location of the unique hues.

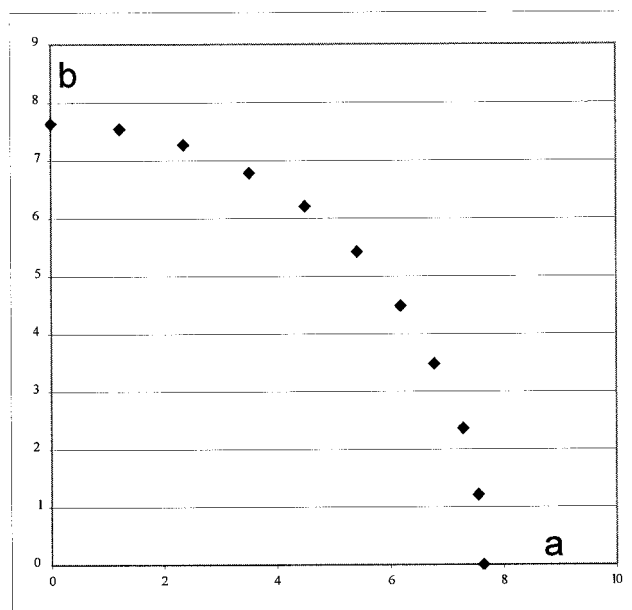


FIG. 5. Hue circle with 10 equally hue-spaced colors in a quadrant, at a given level of chroma derived from the vectors of Fig. 4.

$$\frac{y_n}{r_n + y_n} - \frac{y_{n+1}}{r_{n+1} + y_{n+1}} = \text{const.} \quad (1)$$

where  $y_n$  and  $r_n$  are the estimated percentages of the yellow and red unique hues for color  $n$ . The results according to the two calculation methods differ by a hue angle dependent factor ranging from 0.8 to 1.4. Experimental data do not clearly indicate which approach is the correct one. A final conclusion has important implications for how hue differences should be calculated.

## FUNCTIONS DESCRIBING THE HUE CONTENT

A geometric model for an equally hue-spaced hue circle at equal chroma and lightness based on the CIELAB model (polar coordinates) is a perfect circle with equal division by hue angle showing the location of the individual colors. As mentioned, on the other hand in the Cartesian coordinate system, the locations of the colors when transferred into the polar coordinate system are not equally spaced in terms of hue angle. In both models, one can predict how the hues are spaced on the circle to meet the hypothesis, and what the progression of absolute and relative functions is that result in the perfect circle. In both systems, the distance from the center of the circle to the locus of the color is the chromatic vector, a result of the addition of two unique hue vectors (Fig. 2). The required hue coefficients for ten equal hue steps in a polar system are shown in Fig. 3. The unique hues are represented by those colors consisting of 100% of one hue. The absolute hue functions, indicating the required length of the unique hue vectors in a polar coordinate system, for the complete hue circle are shown in Fig 4, and the resulting placement of the hues in a quadrant of the hue circle in Fig. 5. Placement of forty equal hue steps of a Cartesian system transferred into a polar system is shown in Fig. 2.

The next question to be answered is what psychophysical color functions lend themselves as absolute functions to achieving either kind of spacing for a hue circle. The assumption in opponent-color models is that the opponent-color functions can describe the hue content of mixed hues. Opponent-color functions are the result of subtractions of the cone fundamentals. There is no generally agreed-upon understanding of how the subtraction equations based on cone fundamentals are properly constructed, since there is no accepted model of how cone output interacts in creating

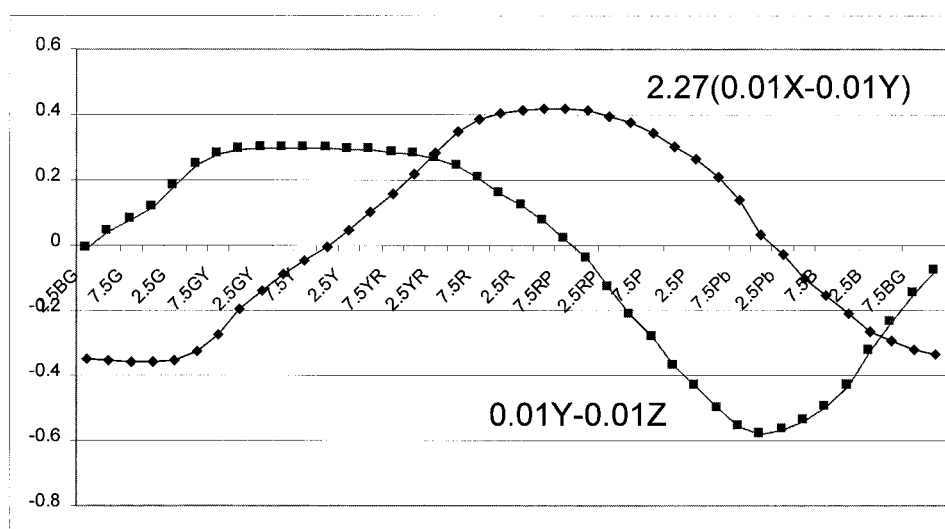


FIG. 6. Chromatic vectors  $a = 2.24 \cdot (0.01X - 0.01Y)$  and  $b = 0.01Y - 0.01Z$  of the Munsell Hue circle at value 6 and chroma 14 (normalized for an equal energy light source). The factor 2.27 balances the area under the curves of the red and green function with that of the yellow and blue function. (Compare to Fig. 4.)

TABLE II. Unique hues expressed as Munsell Hues.

	Implicit in the 2° observer	Experimentally determined
Blue	3.5PB	5PB
Green	2.0BG	3.4BG
Yellow	4.75Y	5Y
Red	8.0RP	1.6R

color perception.<sup>7</sup> However, a model can be based on the CIE colorimetric system. As mentioned before, in an equal lightness plane, when yellowness/blueness of object colors changes, only the  $Z$  value changes; and when redness-greenness changes, only the  $X$  value changes. The effect of subtracting the  $Y$  value from either  $Z$  or  $X$  has, mathematically, merely the effect of normalizing the system so that the neutral point falls onto the origin. If we plot the  $X$  and  $Z$  tristimulus values after subtracting the  $Y$  value, for example for the Munsell 6/14 hue circle (Fig. 6), we find that they vary in a reasonably regular fashion reminiscent of Fig. 4.\* This plot also identifies immediately the unique hues of the standard observer, in this case the 2° observer (Table II). They are similar to unique hues determined by experiment by having observers pick them out of an array of Munsell chips at the same chroma, and within the hue at the same lightness.<sup>†</sup>

The opponent-color functions derived from the color-matching functions (the redness-greenness function multiplied by 2.27 to obtain equal areas under the curves for all four functions) are shown in Fig. 7 on a wavelength scale.

\* The shape of the curves is not affected by the subtraction of  $Y$ ; only the vertical axis changes.

† There is some disagreement in the unique hues implicit in the 2° and the 10° observers, those innate in the observers of the NCS system and of Indow, as well as those experimentally determined in this work. For the difference between the 2° observer and the experiment, see Table I.

What we must achieve is to convert them to a hue scale so that they approach as closely as possible the functions of Fig. 4.

When we construct the hue circle from the  $X$ - $Y$  (a) and  $Y$ - $Z$  (b) chromatic vectors for the Munsell Renotations, we find a distorted circle [Fig. 8(a)]. It is distorted in a different manner when using the CIELAB relationship [Fig. 8(b)]. It is evident from the chroma steps of the near-unique Munsell Hues that the unique hue vectors do not change linearly as a function of chroma. But uniform application of cube root power is not the answer either. If the chromatic vectors of mixed hues are the sum of the two unique hue vectors, the unique hue vectors at different chromas must be linearized to obtain a hue circle. Linearization as a function of chroma of only the unique hue vectors automatically adjusts those of the mixed hues in the right proportion, assuming that there are no additional effects.

### LINEARIZATION OF THE UNIQUE HUE CHROMA SCALES

The linearization power that is used in the CIELAB formula is the cube root. It is derived from the close approximation of the cube root function to the Munsell value function. The idea that the same linearization power should also be applied to the  $X$  and  $Z$  tristimulus values derives from the Adams-Nickerson color space and difference formulas. I am not aware of independent confirmation of this assumption.

If we plot the  $a$  values for the red and green near-unique hues at increasing chroma [Fig. 9(a)], and the  $b$  values for the near-unique yellow and blue chroma steps [Fig. 9(b)], we find that the power required to linearize the  $a$  and  $b$  functions differs. The optimum power functions for the four scales are listed in Table III, which also contains the optimum functions for the 10° observer, and

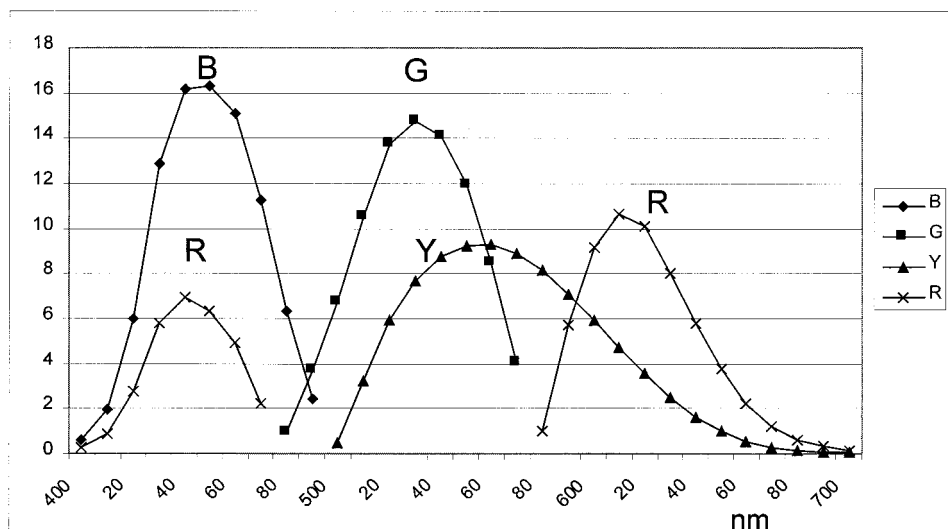
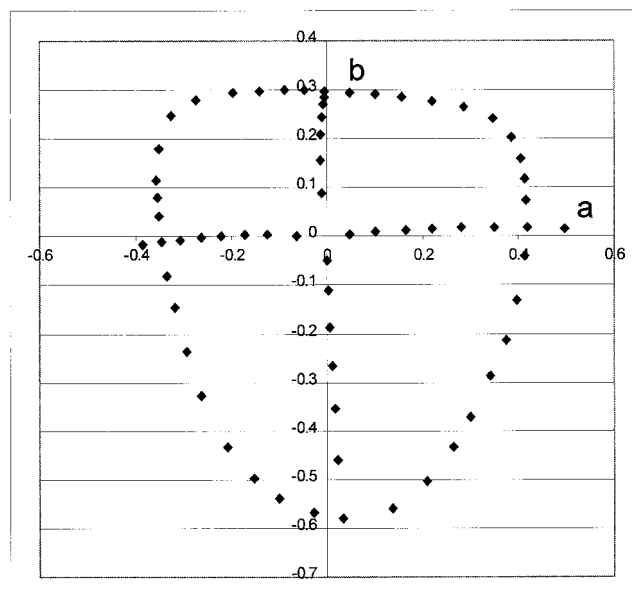
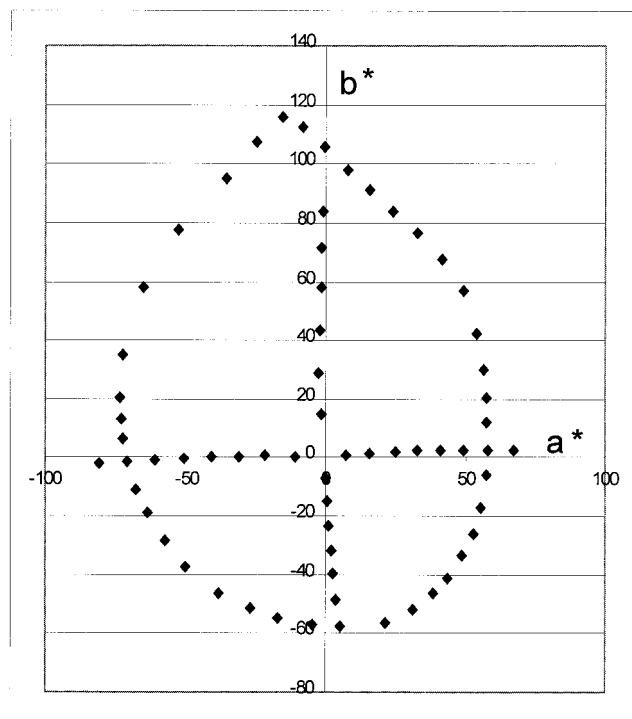


FIG. 7. Opponent-color functions derived from subtraction of CIE 2° color-matching functions. All lobes are shown positive for ease of comparison.  $a = 2.24(\bar{x} - \bar{y})$ ,  $b = \bar{y} - \bar{z}$ .



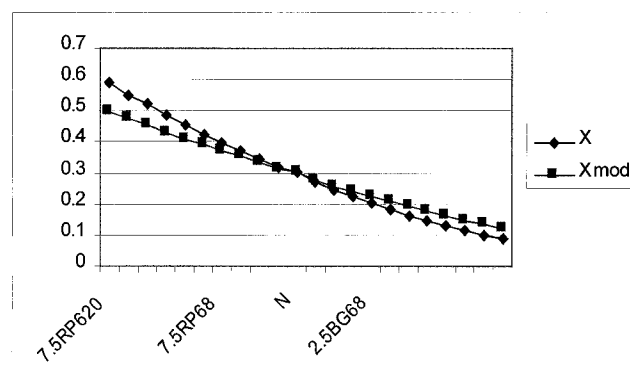
(a)



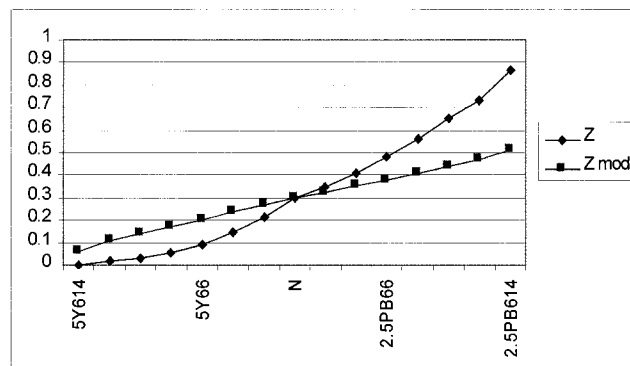
(b)

FIG. 8. (a) Munsell Hue circle at value 6 and chroma 14 in the linear model.  $a = 2.24(\bar{a}_x - \bar{x})$ ,  $b = \bar{y} - \bar{z}$ . (b) Same Munsell hue circle as Fig. 7, but in the CIELAB  $a^*$ ,  $b^*$  diagram.

the OSA-UCS colors<sup>8</sup> at  $L=0$ , and for the NCS system. The values are somewhat different, but with the same general tendencies. This is quite remarkable, because the three systems have been derived by widely different methodologies. It should be mentioned that the gamut covered by OSA-UCS colors is somewhat smaller than



(a)



(b)

FIG. 9. (a)  $0.01X$  and modified  $X$  as a function of the near-unique hues 7.5RP and 2.5BG at chromas from  $N$  to the limit defined in the Munsell Renotations at value 6. The modification involves application of the power 0.75, balanced at  $N$ , to linearize the function. (b)  $0.01Z$  and modified  $Z$  as a function of the near-unique hues 5Y and 5PB at chromas from  $N$  to 14, at value 6. The modification involves application of the power 0.333 to the yellow portion and of power 0.5 to the blue portion, balanced at  $N$ , to linearize the function.

that of the Munsell Renotations, and that also for the Munsell red-green scale a linear relationship is satisfactory from chroma 0 to 8.

There is an additional problem that requires solving, however. Plots of the near-unique blue Munsell color 5PB at increasing chroma and of nearby hues show that, as a function of increasing chroma and decreasing lightness, the

TABLE III. Optimum formula parameters for the Munsell, OSA-UCS and NCS color spaces.

	Munsell	OSA-UCS	NCS
Power, blueness	0.5	0.5	0.75
Power, yellowness	0.333	0.4	0.333
Power, redness-greenness	0.75	1	0.75
$Z$ factor, redness-greenness <sup>a</sup>	0.018	0.10	—
Ratio R/G to Y/B	1.67:1	1.2:1	1.5:1

<sup>a</sup> Factor by which  $Z$  is subtracted from to straighten the blue constant hue lines, at  $Y = 30$ . For the Munsell Renotation data there is a slight dependency of the factor on  $Y$ ; not so for the OSA-UCS data.



hue lines curve toward redness. Figure 10 shows the relative  $X$  values of 5PB as a function of value and chroma. The curvature is virtually identical in a linear system and in the CIELAB system. A similar but more distinct curvature exists in the OSA-UCS system. There, the curvature is already distinct at  $L = 0$  [which is close to  $V = 6$ , see Fig. 12(a)].<sup>‡</sup> This implies that the blue colors seen as having identical hues in the OSA-UCS are not the same as those in the Munsell system, particularly at higher chroma. (In the NCS system, unique blue is greenish and varies in the  $a^*$ ,  $b^*$  diagram as a function of saturation and blackness. At higher chroma, the curling is toward more greenness.) A redetermination of constant hue blue colors seems required. The basic problem has also surfaced in small color-difference evaluation, where unit ellipses in the  $a^*$ ,  $b^*$  diagram in this area are angled towards redness at higher chroma, in line with the curvature of the equal hue line.<sup>9</sup> The curvature of the unique blue chroma line can be eliminated by subtracting a small fraction of the  $Z$  value from the  $X$  value. The implication is that the short wave hump of the  $\bar{x}$  color-matching function is slightly too large. A somewhat different transformation of the  $\bar{x}$  color-matching function may be required to eliminate the curvature directly. The value for the fraction of  $Z$  is slightly dependent on  $Y$  in the Munsell Renotations, but not in OSA-UCS.

The formulas for the linearized  $a$  and  $b$  values for the Munsell system, including the blue correction, are as follows:

$$a^\wedge = \frac{600}{0.133Y^{0.59}} \left[ \left( 1 + \frac{0.1}{Y^{0.5}} \right) * \left( \frac{X}{X_0} \right)^{0.75} * \left( \frac{Y}{Y_0} \right)^{0.25} - \left( \frac{Y}{Y_0} \right) - \left( \left( \frac{0.1}{Y^{0.5}} \right) * \left( \frac{Z}{Z_0} \right) \right) \right]$$

if  $Y_n > Z_n$

$$b^\wedge = \frac{340}{0.133Y^{0.59}} \left[ \left( \frac{Y}{Y_0} \right) - \left( \left( \frac{Z}{Z_0} \right)^{0.333} * \left( \frac{Y}{Y_0} \right)^{0.667} \right) \right] \quad (2)$$

if  $Z_n > Y_n$

$$b^\wedge = \frac{380}{0.133Y^{0.59}} \left[ \left( \frac{Y}{Y_0} \right) - \left( \left( \frac{Z}{Z_0} \right)^{0.5} * \left( \frac{Y}{Y_0} \right)^{0.5} \right) \right]$$

$Y_n$  and  $Z_n$  are normalized tristimulus values, i.e., comparable to  $Y/Y_0$ , (and similarly for  $Z$ ); they correspond to an equal energy light source. The caret designator is used to distinguish these values from the linear or the cube root values. The multipliers have been chosen so that, on average,  $a$  and  $b$  values approximately equal to those resulting from application of the CIELAB formula are obtained. The

<sup>‡</sup> In the OSA-UCS formula, the problem has been solved by a peculiar choice of cone fundamentals. When plotting Munsell colors at value 6 in the  $j, g$  diagram of OSA-UCS, the curvature of the blue colors is reversed. In general, the OSA-UCS formula suffers from the same cube-root-related problems as the CIELAB formula.

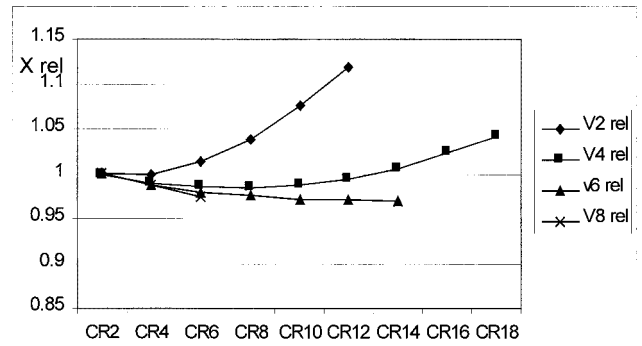


FIG. 10. Relative  $X$  values of Munsell color 5PB as a function of value and chroma.

$Y$ -based multipliers for  $X$  and  $Z$  are required to result in values of 0 for the  $X$  and  $Z$  functions at the neutral point.

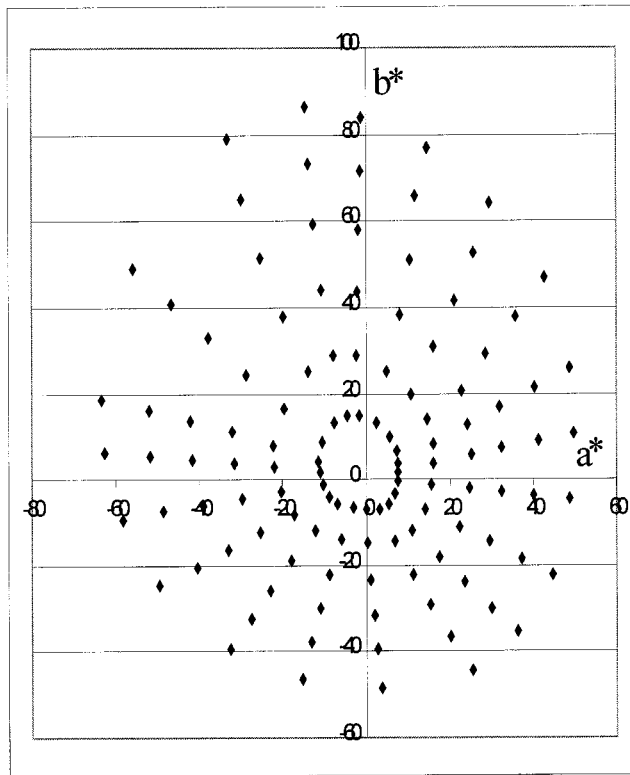
One of the advantages of a cube root formula is that it results in closely similar  $a$  and  $b$  values regardless of lightness for colors seen as having the same chroma. (It converts the conical form of the linear  $Lab$  space to a cylindrical form.) A somewhat more complicated denominator had to be found to accomplish the same result.

When applying the formulas to the Munsell Hue circles at 6/8, 8/8, and 3/8 a contour much closer to a circle is obtained. [Fig. 11(a–f)]. Also, the OSA-UCS [Fig. 12(a,b)] and the NCS spacings (Fig. 13(a,b)), with appropriate power functions, are much improved over those obtained with a linear formula or the CIELAB formula. We notice, however, that the Munsell hues on that circle are quite unevenly spaced, as in the  $a^*$ ,  $b^*$  diagram.

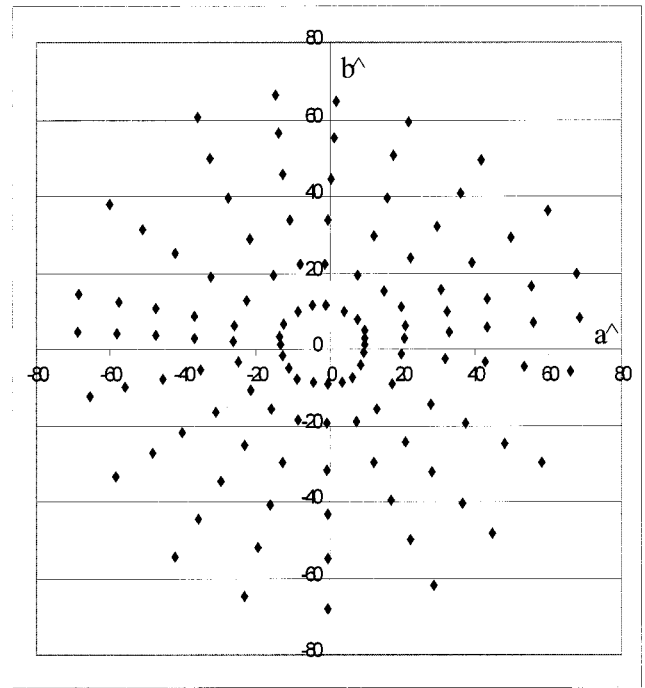
#### IS THE MUNSELL HUE CIRCLE VISUALLY EVENLY SPACED?

This question has been addressed informally and formally in the past. A multi-dimensional scaling experiment by Indow and Ohsumi has indicated significant discrepancies in the red to blue sector.<sup>10</sup> Not being aware of any published direct testing of the uniformity of a Munsell Hue circle, I have performed a small experiment involving six observers to identify shortcomings, if any, of the scaling of the Munsell Hue circle at value 6 and chroma 8. There is no claim made that the results of the following experiment are fully representative of the average observer. They are meant as indicative of apparent problems with the Munsell System Hue scale that need to be resolved through more extensive experiments with more observers before a significantly improved color-space formula can be recommended for general use.

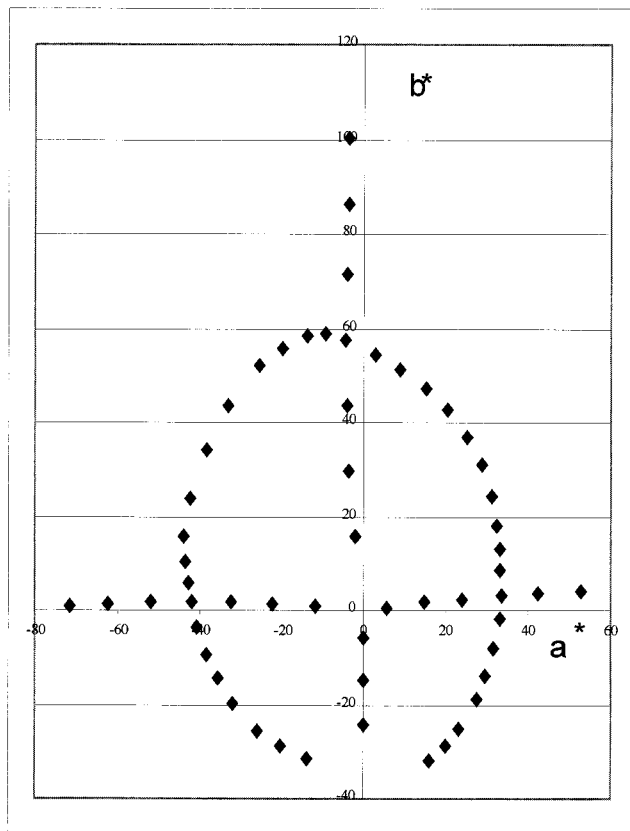
The chip pair of 5PB and 10B was used as hue difference standard. The chips were displayed on a neutral background of  $N=6$ . Pairs of chips of other hues around the hue circle were presented, and all chips were covered with a Color-curve<sup>®</sup> grey mask<sup>11</sup> (close to  $N=6$ ), so that four separated circular patches at 14-mm diameter of color were visible



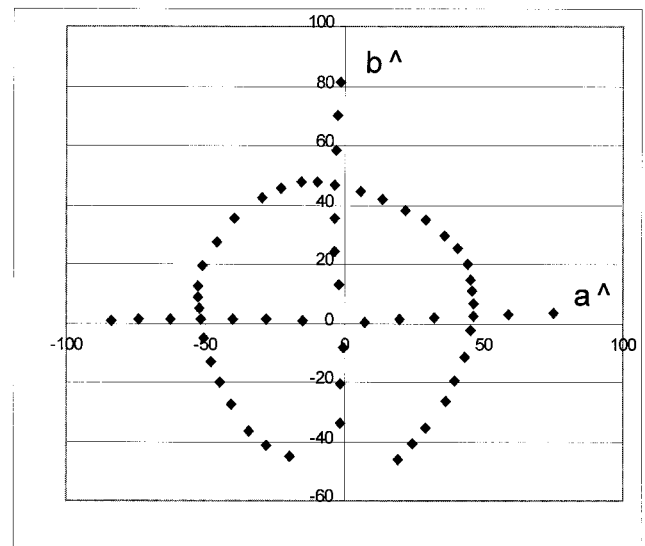
(a)



(b)



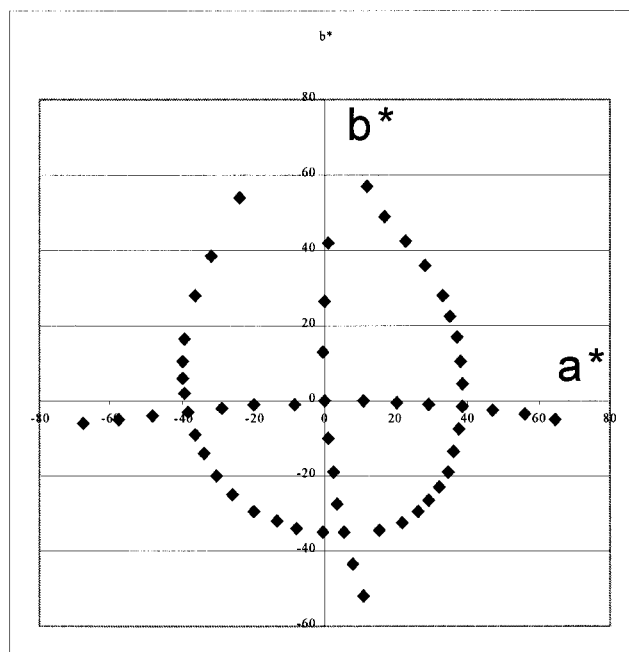
(c)



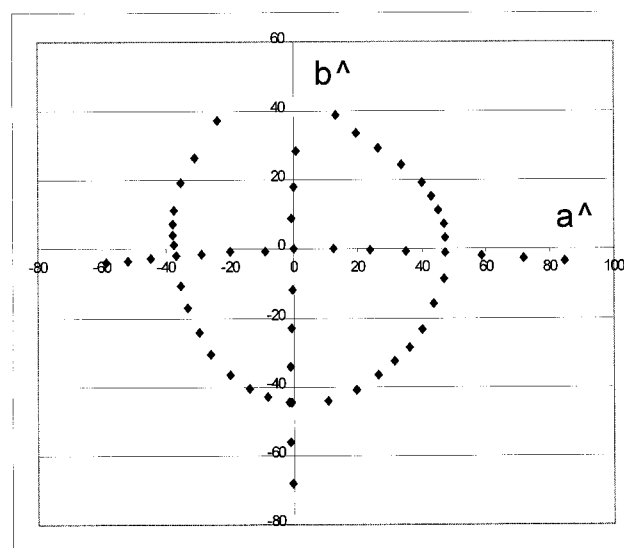
(d)

FIG. 11. (a) Every second Munsell hue at value 6 and chromas 2–12. Coefficient of variation of the 120 chroma differences is 21.7%. (b) Munsell data from Fig. 11(a) in the  $a^b^$  diagram. Coefficient of variation of the 120 chroma differences is 8.3%. (c) Munsell Hue circle and chroma steps of near-unique hues at value 8, chroma 8 in the  $a^*, b^*$  diagram. (d) Munsell data from Fig. 11(c) in the  $a^b^$  diagram.





(e)



(f)

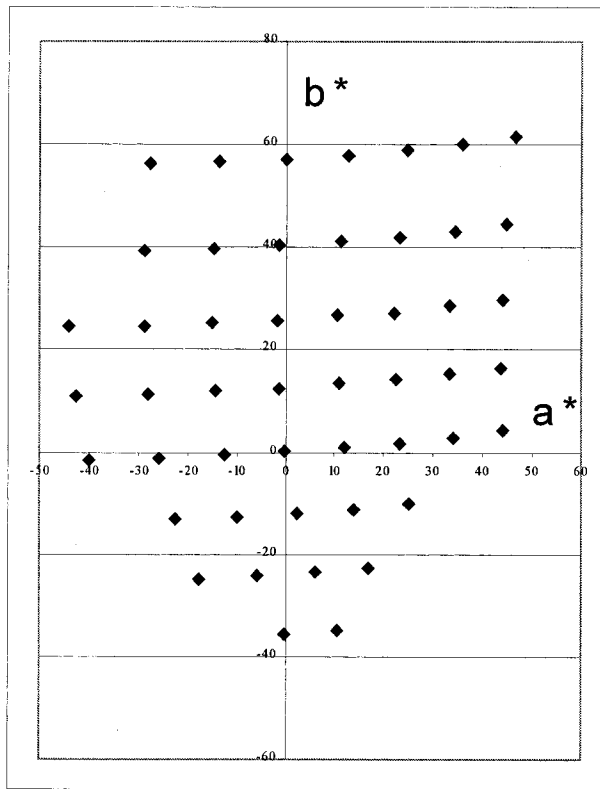
FIG. 11. (Continued) (e) Munsell hue circle and chroma steps of near-unique hues at value 3, chroma 8 in the  $a^*$ ,  $b^*$  diagram. (f) Munsell data of Fig. 11(e) in the  $a^\wedge$ ,  $b^\wedge$  diagram.

against an  $N=6$  background and with 6-mm separation between the patches (Fig. 14). The observer judged if the hue difference between the standard and the sample pair was equal or unequal. Based on the first judgment, one of the two sample chips was replaced for a new judgment. The final result of the judgment was that the standard hue difference was either equal to the hue difference between chips  $a$  and  $b$ ,  $a$  and  $c$ , or equal to the difference between  $a$  and halfway between  $b$  and  $c$ , where  $a$ ,  $b$ , and  $c$  are chips of the 40-step Munsell Hue scale at value 6 and chroma 8. No closer judgment than a half-step between two adjacent Munsell 40 hue chips was asked for. There was no case where an observer determined the standard hue difference to be smaller than a single step difference in adjacent Munsell 40 hue chips. Six observers made judgments around the complete hue circle in this fashion on two different occasions. Two observers repeated the experiment using chips 5Y6/8 and 10Y6/8 as standard pair. About half the judgments were made in natural north sky daylight on a moderately overcast day, the remainder under Macbeth D65 illumination. When analyzing the judgments made in daylight and under artificial illumination separately, no trend was noticeable. The judgments against the yellow standard pair showed minor differences compared to those against the blue standard pair, and they were excluded. The results of the twelve judgments were averaged. They are shown in Table III, which lists the means, expressed as Munsell hue values, their standard deviations, and the step differences. The unique hues had been determined by a group of 15 observers separately in an earlier experiment.<sup>6</sup> The means were converted to chromaticity values by interpolation of Munsell Renotation data.

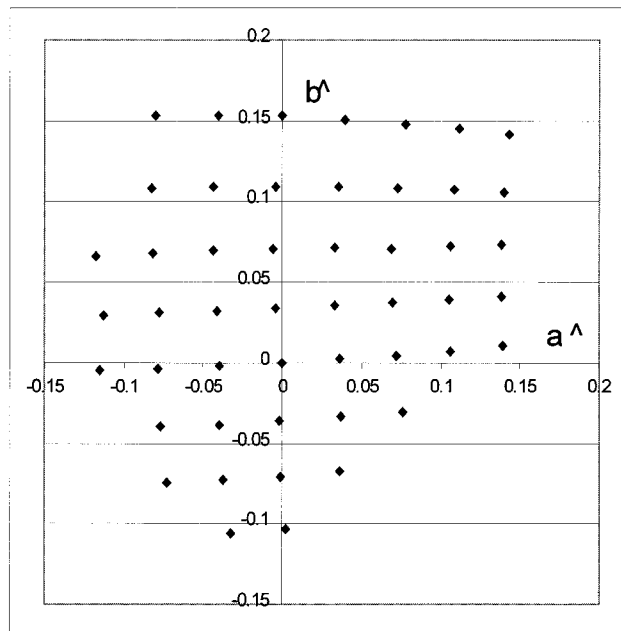
(The unique hues were also extrapolated to higher and lower chromas by interpolation of the Munsell Renotations at those chromas.) In different areas around the circle, the 5.0 Munsell 100 step difference of the standard pair was seen equal to from 3.0 to 5.8 steps. The averages were minimally adjusted to result in round numbers of equal steps between unique hues. (It is not obvious that there should be integer numbers of equal-sized steps in the four quadrants. More extensive experimental work is required to come to a conclusion in this matter.) That 22 equal steps were found is an artifact of the choice of the standard pair.

Of particular interest is the number of equal hue intervals, as determined in this experiment, between unique hues. It should be mentioned that, while for three of the four unique hues the observers were in good agreement with the 2° standard observer, there is a noticeable difference in case of the red unique hue. (Approximately the same difference applies to the unique red hue in the NCS system.) Table IV compares the hue steps found in the experiment against those of the Munsell 40 hue color circle. The experimental steps are, of course, on average about twice the size of a Munsell 40 hue step. While in three of the four quadrants there is reasonable agreement, in the red to blue quadrant the experiment shows relatively about 30% more steps than in the Munsell System. This is not totally surprising in the light of the earlier mentioned findings by Indow and Ohsumi. In fact, there is a significant level of agreement between the two sets of data.

Apparently, phenomenologically the four unique hues are not equally spaced (in terms of an equal number of equal-sized hue steps between them). Unique blue and green



(a)



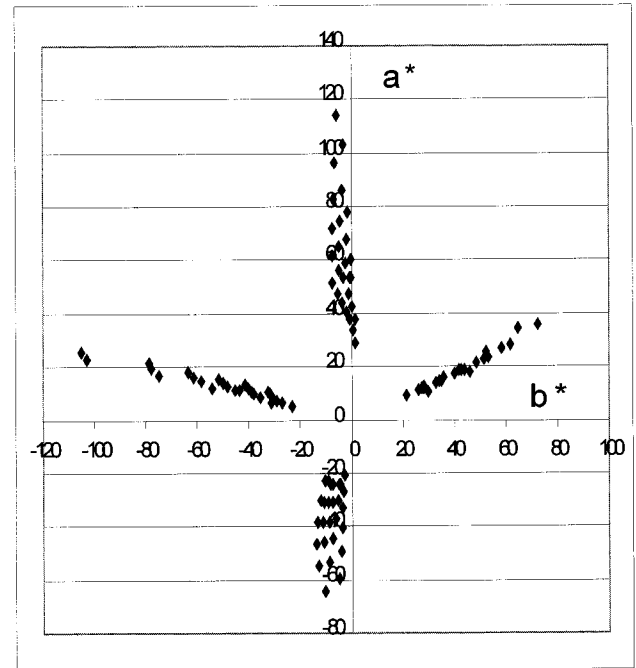
(b)

FIG. 12. (a) OSA-UCS colors at  $L=0$  in the  $a^*, b^*$  diagram. (b) The colors of Fig. 10(a) in the  $a^{\wedge}, b^{\wedge}$  diagram.

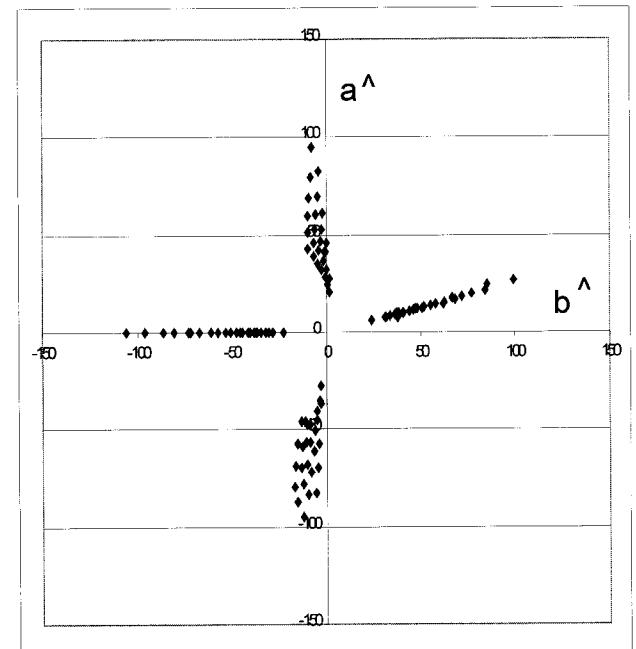
appear phenomenologically less distant from each other than blue and red. There is no immediately apparent explanation for the cause of this difference.

The 22 equal hue-step colors and extrapolated unique

hues were plotted in the  $a^*, b^*$  diagram [Fig. 15(a)], as well as in the  $a^{\wedge}, b^{\wedge}$  diagram [Fig. 15(b)]. In Table V, a comparison of the corresponding average hue and chroma differences is listed. It is evident, that the  $a^{\wedge}, b^{\wedge}$  diagram offers significant improvement in both areas. The improvement indicates that the  $a^{\wedge}, b^{\wedge}$  diagram may be a uniform chromatic diagram. When plotting the absolute  $a^{\wedge}, b^{\wedge}$  values of



(a)



(b)

FIG. 13. (a) All NCS colors of the unique hues in the  $a^*, b^*$  diagram. (b) The NCS colors of Fig. 11(a) in the  $a^{\wedge}, b^{\wedge}$  diagram.

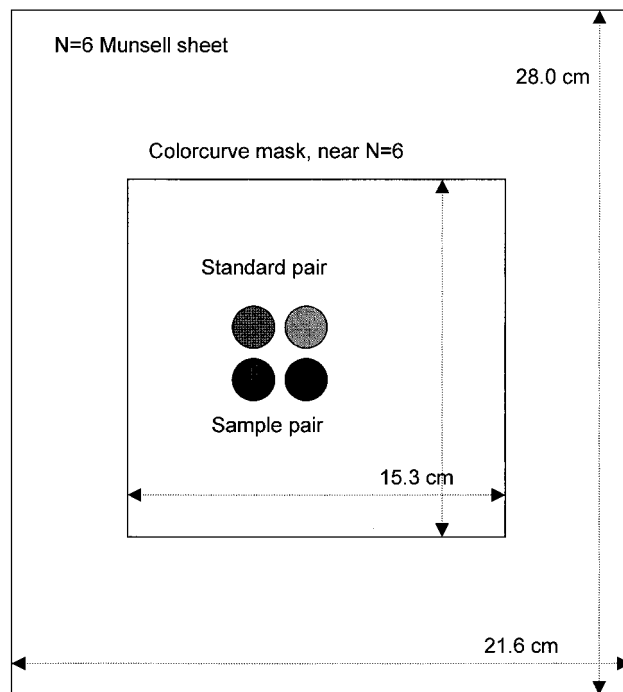


FIG. 14. Physical arrangement of the hue spacing experiment. (See text for details.)

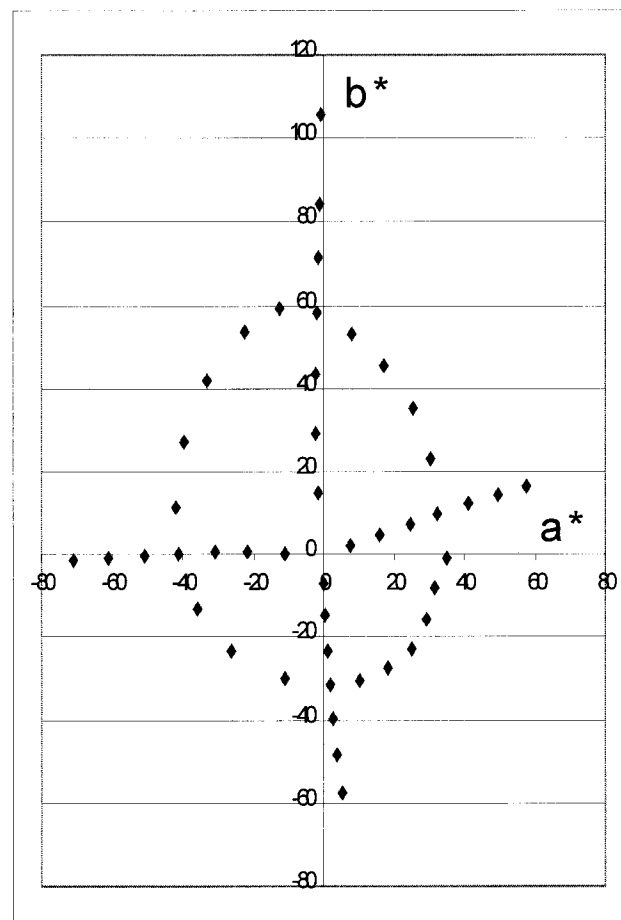
the 22 visually equally spaced hues on a hue scale (Fig. 16), the result is quite close to the ideal form of Fig. 4. Similarly, the calculated hue coefficients for these colors approach the ideal distribution (Fig. 17). The discrepancies in parameters based on the three different sets of data (Munsell, OSA-UCS, NCS) must be resolved in additional visual experiments, as must be the question of what are constant hue blue colors.

#### ADAPTATION EFFECTS RELATED TO COLOR DIFFERENCES

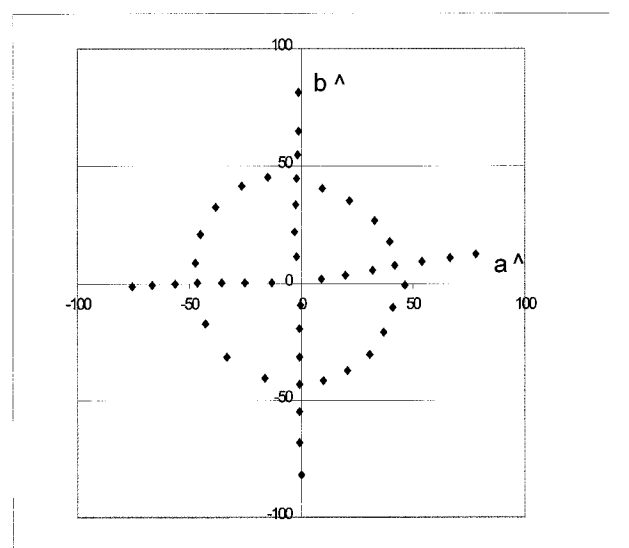
In the Munsell system, colors varying in hue but of equal chroma by definition are equidistant from neutral gray. In the  $a^*$ ,  $b^*$  diagram, Munsell colors with double the chroma have chromatic vectors double in length. This is quite remarkable, given the simplicity of the model. The chroma scale, as the hue scale, is based on adaptation to a neutral gray background, and the simple model can represent this situation well. This no longer applies when we judge relatively small differences. Here the results are known to be

TABLE IV. Relative number of equal hue steps in the Munsell and NCS systems, and experimentally determined.

Quadrant	Munsell	NCS	Experimental
Red to yellow	1	1	1
Yellow to green	0.98	1.13	1.2
Green to blue	0.75	1.13	0.8
Blue to red	0.84	1.63	1.4



(a)



(b)

FIG. 15. (a) Twenty-two experimentally equally hue-spaced Munsell colors at value 6 and chroma 8 and additional chroma steps of the experimentally found unique hues in the  $a^*$ ,  $b^*$  diagram. Chromaticity coordinates were interpolated from Munsell Renotation data. (b) The colors of Fig. 15(a) in the  $a^\wedge$ ,  $b^\wedge$  diagram.

TABLE V. Average hue and chroma differences and their coefficients of variation for 22 experimentally determined hue differences and 24 chroma differences in the  $a^*$ ,  $b^*$  diagram and the  $a^\wedge$ ,  $b^\wedge$  diagram.

	Hue differences		Chroma differences	
	Average	Coeff. of Var., %	Average	Coeff. of Var., %
CIELAB	11.5	23.4	10.4	30.1
$a^\wedge$ , $b^\wedge$ formulas	11.6	13.2	11.4	14.5

affected by the surround. Color difference perception is most sensitive, if the surround is close in hue, chroma, and lightness to the two colors being compared for differences, i.e., when the visual system is adapted to a surround similar to the samples being compared. This affects all three visual attributes: hue, chroma, and lightness. The normal industrial situation for visually evaluating color differences is against a light, neutral gray surround (in a light booth). This surround is similar to that used in establishing the Munsell system. The perception of hues should not be different in the Munsell system and in hue difference evaluation in a light booth. If the  $a^\wedge$ ,  $b^\wedge$  diagram is hue uniform, no adjustment of hue differences is required (except perhaps when evaluating small color differences of adjacent samples). But the perception of chroma and lightness differences will be affected. The closer the chroma and lightness of the samples being compared is to the gray background, the larger are the perceived differences. The Munsell Chroma and Lightness scaling needs adjustment for the purpose of small color

TABLE VI. Number of equal hue steps and ratios between unique hues in the Munsell System and experimentally determined.

Quadrant	B-G	G-Y	Y-R	R-B
Munsell 40-step ratio	8.5	11.5	9.5	10.5
Experimental ratio	1	1.35	1.12	1.24
Experimental ratio	4	6	5	7
Experimental ratio	1	1.5	1.25	1.75

difference calculation.\* The adaptation adjustment factors in CMC and similar color difference formulas have been introduced to achieve this. There is no agreement at this time on the exact values for  $S_L$  and  $S_C$ . The hue difference adjustment factor  $S_H$  in CMC has a chroma-dependent component and a hue angle-dependent component. The former adjusts hue differences to be in line with adjusted chroma differences; the latter adjusts the CIELAB hue differences to be in better agreement with those derived from the Coats acceptability data. The current recommendation in CIE94 is limited to the chroma-dependent factor. Different factors have been proposed for the pure hue correction and agreement has not yet been reached.<sup>12</sup> A factor  $S_H$  may no longer be required for a color-difference formula based on  $a^\wedge$ ,  $b^\wedge$  type formula, while  $S_L$  and  $S_C$  are.

There is some concern among experts about the fact that introduction of such factors means that the formulas no longer represent a color space. It appears possible to incorporate the  $S_C$  adjustment into the power functions that relate

\* I have proposed a cube-root formula with an  $S_C$  type correction for color difference calculation 26 years ago. (Kuehni R. Color difference and objective acceptability evaluation. J Col Appear (1972);1(3):4-10.)

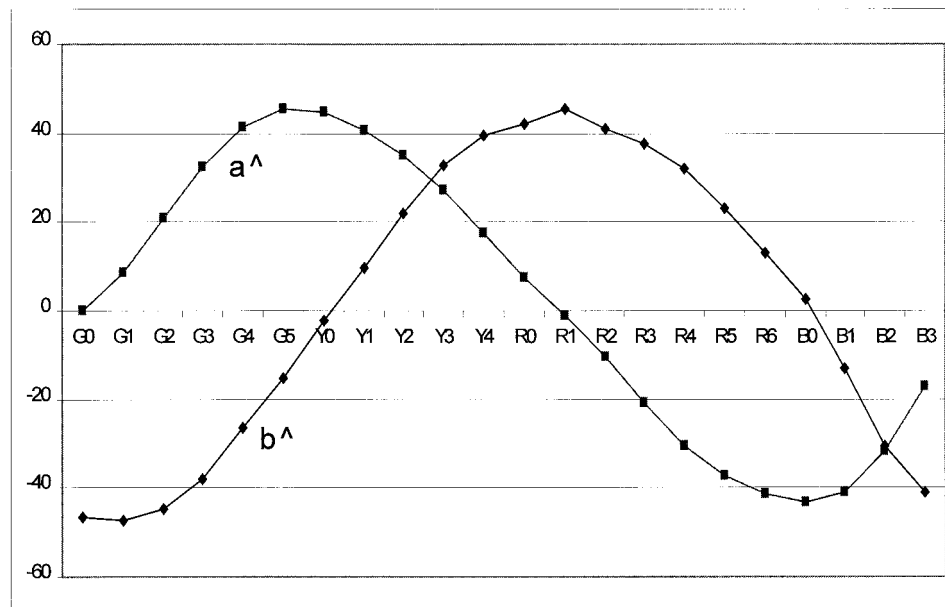


FIG. 16. The  $a^\wedge$  and  $b^\wedge$  chromatic vectors of the 22 experimentally equally hue-spaced colors as a function of hue. (Compare with Fig. 4.)

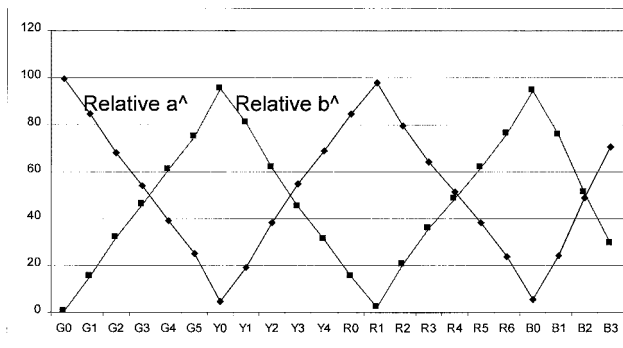


FIG. 17. Hue coefficient diagram of the 22 experimentally equally hue-spaced colors as a function of hue. (Compare with Fig. 3.)

the  $a$  and  $b$  values to chroma. The lightness crispening effect can be handled as in the OSA-UCS formula. A color space for small color differences based on a gray surround of a particular lightness appears possible.

### CONCLUSION

I have shown that a single linearizing power for the opponent-color functions is incorrect, and that hue and chroma spacing is much improved by using optimized linearizing powers. This finding is valid for three sets of “uniform” color-space data established under widely varying concepts. The formulas fitted to the Munsell Renotations have been presented. If the Renotations or another set of uniform color-space data will provide an improved basis formula for

small color-difference calculation remains to be seen. Using the same concept, formulas can be directly optimized to small color-difference data for improved correlation between visual and calculated data.

1. For example: Vos JJ, Walraven PL. An analytical description of the line element in the zone-fluctuation model of colour vision. *Vision Res* 1972;12:1327–1365.
2. Kuehni RG. The conundrum of supra-threshold hue differences. *Col Res Appl* 1998;23:335–336.
3. Marcus RT. The measurement of color. In: Nassau K, editor. *Color for science, art and technology*. Amsterdam: Elsevier; 1998.
4. Indow T. Predictions based on Munsell notation. II. Principal hue components. *Col Res Appl* 1999;24:19–32.
5. Natural Color System (NCS). Swedish Standard SS01 91 00, as described by: Hård A, Sivik L, Tonnquist G. NCS natural color system, from concepts to research and applications, Part I and Part II. *Col Res Appl* 1996;21:180–220.
6. Kuehni RG. Hue uniformity and the CIELAB space and color difference formula. *Col Res Appl* 1998;23:314–322.
7. Lee BB. Receptors, channels and color in primate retina. In: Backhaus WGK, Kliegl R, Werner JS, editors. *Color vision*. Berlin: Walter de Gruyter; 1998.
8. OSA-UCS and Munsell Renotations, as published in: Wyszecki G, Stiles WS. *Color science*, 2<sup>nd</sup> ed. New York: Wiley; 1982.
9. Melgosa M, Hita E, Poza AJ, Alman DH, Berns RS. Suprathreshold color-difference ellipsoids for surface colors. *Col Res Appl* 1997;22: 148–155.
10. Indow T, Ohsumi K. Multidimensional mapping of sixty Munsell colors by nonmetric procedure. In: Vos JJ, Walraven PL, editors. *Color metrics*. Soesterberg: Netherlands Inst Percep; 1972.
11. Colorcurve® System, Colorcurve Systems Inc., Minneapolis 55401.
12. Qiao Y, Berns RS, Reniff L, Montag E. Visual determination of hue suprathreshold color-difference tolerances. *Col Res Appl* 1998;23: 302–313.